

Original Research Article

TEMPORAL AND SPATIAL VARIATION OF THE VIRTUAL HEIGHT OF IONOSPHERIC F2-LAYER OVER TWO EQUATORIAL STATIONS DURING MINIMUM TO ASCENDING PHASE OF SOLAR CYCLE 25

ABSTRACT

Introduction: The research examines ionospheric F2-layer virtual height (h'F2) variations at Ilorin (14.80°N, 17.40°W) in the Africa sector and Boa Vista (2.80°N, 299.30°E) in the America sector, during Solar Cycle 25's minimum and ascending phases.

Aims: The aim is to investigate the temporal and spatial variations of the virtual height of the F2-layer over two equatorial stations during the minimum to ascending phase of Solar Cycle 25 at two equatorial stations in two different longitudinal sectors.

Methodology: Analyzing data from these stations statistically, the paper investigates diurnal, seasonal, and annual variations in h'F2.

Results: Diurnally, the h'F2 demonstrates greater responsiveness during daytime (06:00 – 18:00 LT) compared to nighttime (18:00 – 05:00 LT). Seasonally, peak values occur around noon and post-noon periods, displaying significant disparities during equinoxes and solstices over both stations in the different solar phases. During the minimum phase year (2020), peak heights of h'F2 ~~reach~~ ~~reached~~ 387 km at Ilorin and 372 km at Boa Vista. ~~In the~~ ~~During~~ ascending phase year (2021), these peaks slightly ~~shift~~ ~~shifted~~ to 389 km at Ilorin and 404 km at Boa Vista. Annually, the highest peak values of h'F2 occur at noon, measuring 376 km at Ilorin and 331 km at Boa Vista during the minimum phase, while during the ascending phase, both stations recorded almost identical values of 305 km at noon. Overall, h'F2 variation exhibited higher magnitude at Ilorin in the African longitudinal sector than at Boa Vista in the American longitudinal sector during the minimum phase of solar cycle 25, with the reverse observed during the ascending phase.

Conclusion: This detailed analysis illuminates the complex variations in ionospheric behavior across various timeframes and geographic locations, showcasing substantial variability and sensitivity to solar influences in equatorial stations across Africa and America.

Comment [SK1]: Just make one paragraph.

Keywords: Variability, Virtual Height, Minimum and Ascending Solar Phase, Solar Cycle 25.

1. INTRODUCTION

The ionosphere, situated in the upper atmosphere of Earth, plays a vital role in various phenomena such as radio wave propagation, satellite communication, and space weather dynamics [1 – 5]. Among its layers, the F2-layer holds particular significance in long-distance radio communication. Understanding the dynamic changes in its virtual height over equatorial regions throughout the solar cycle is imperative for predicting and mitigating potential disruptions to navigation and communication systems [6 – 10]. The F2-layer, positioned approximately 200 to 500 kilometers above Earth's surface, is a notable layer of the ionosphere. This layer, along with others, constitutes the ionosphere—a region of the upper atmosphere ionized by solar and cosmic radiation [10 – 11]. The F2-layer stands out for its notable electron density, peaking typically during daytime owing to solar radiation's

ionizing effects. Its significance lies in facilitating long-distance ~~high-frequency~~high-frequency (HF) radio communication by reflecting radio waves back to Earth's surface, enabling over-the-horizon communication [12 – 13]. However, the F2-layer's characteristics, including electron density and altitude, exhibit variability influenced by factors like solar activity, time of day, and geographical location. These variations exert substantial influence on radio propagation conditions, underscoring the F2-layer's pivotal role in radio communication systems and ionospheric modeling [14 – 16].

Ionospheric parameters used in studying the ionosphere F2-layer behaviour include the critical frequency of the F2 –layer (foF2), ~~the~~ maximum electron density of the F2-layer (NmF2), ~~the~~ virtual height of the F2-layer (h'F2), ~~the~~ maximum height of the F2-layer just to mention but a few. The virtual height of the ionosphere signifies the perceived altitude at which an electromagnetic wave undergoes reflection by the ionospheric layer. It is termed "virtual" because it represents the effective altitude observed by the incoming wave, influenced by the refractive characteristics of the ionosphere [17- 19].

The equatorial region outlines the vicinity encircling Earth's equator, the imaginary line dividing the planet into Northern and Southern Hemispheres. Extending across several degrees of latitude on either side of the equator [20 – 2], this zone shows distinct climatic features owing to its proximity to the equator. Warm temperatures, high humidity levels, and relatively consistent day lengths throughout the year characterize the equatorial region. Vital to identifying an equatorial area is the Equatorial Ionization Anomaly (EIA), a remarkable feature of the ionosphere exhibiting asymmetrical plasma density distributions in the F-region. The dynamic interplay of solar forcing, geomagnetic influences, and atmospheric dynamics induces significant variations in the virtual height of the F2-layer, nestled within the EIA [23 - 26]. These solar-driven variations greatly impact ionospheric plasma density and electron dispersion, particularly at equatorial latitudes where the Earth's magnetic equator intersects with geomagnetic field lines [27].

The solar cycle, a recurring pattern lasting approximately 11 years, represents the cyclic flux in the Sun's activity. Variations in sunspots, solar flares, and other solar phenomena characterize this cycle [28 – 29]. At the core of this phenomenon is the Sun's magnetic field, which undergoes complete polarity reversal roughly every 11 years, driving the solar cycle [30]. The solar cycle manifests in distinct phases of high activity (solar maximum) moderate activity (ascending or descending solar phase) and low activity (solar minimum) throughout its progression [31]. Comprehending the solar cycle is overbearing for studying space weather, solar Physics, and potential impacts on Earth's climate and technology [32]. Currently, Solar Cycle 25 commenced around December 2019 and is anticipated to extend until approximately 2030. This cycle succeeded Solar Cycle 24, spanning roughly from 2008 to 2019. While solar cycles typically endure around 11 years, their exact duration may vary [33]. The present transition from solar minimum to the ascending phase marks Solar Cycle 25. Throughout this period, solar activity has been progressively intensifying, leading to fluctuations in solar irradiance, solar wind dynamics, and geomagnetic activity [28]; [34]; [3]. Studying the variations in the virtual height of the F2-layer across equatorial stations provides insights into the underlying mechanisms driving ionospheric dynamics throughout the solar cycle. Comparing observations from stations at different longitudes allows for the identification of longitudinal changes and assessment of how factors like geomagnetic declination and local time influence ionospheric variability. This analysis is crucial for enhancing ionospheric models, improving space weather forecasting, and ensuring the reliability of communication and navigation systems operating in equatorial regions. By deepening our understanding of ionospheric ~~Physies~~physics and its implications for technology applications and space weather forecasting efforts, the findings from this investigation contribute to advancements in these critical fields.

In this study, we aim to investigate the temporal and spatial variations of the virtual height of the F2-layer over two equatorial stations during the minimum to ascending phase of Solar Cycle 25 at two equatorial stations in two different longitudinal sectors.

2. MATERIAL AND METHODS

2.1 Data Source

The data used in this research are the hourly monthly mean h'F2 experimental data observed at Ilorin, (~~Geographical Latitude~~ 14.80 °N, ~~Geographical Longitude~~ 17.40 °W) in the African longitudinal sector and Boa Vista, (~~Geographical Latitude~~ 2.80 °N, ~~Geographical Longitude~~ 299.30 °E) in the American longitudinal sector, during ~~ascending phase solar cycle 25 (year 2020 – 2021)~~ ~~minimum phase year 2020 and ascending phase year 2021~~ of solar cycle 25 with Zurich sunspot number Rz = 7.9 and 32.9 respectively. The Zurich sunspot number (Rz) data were used as ~~an~~ index of solar activity for each of the ~~year~~ years. The observed h'F2 ionosonde data obtained from the DPS digisonde at Ilorin and at Boa Vista were archived at Global Ionospheric Radio Observatory (GIRO) with website <https://giro.uml.edu/didbase/scaled.php>. The Rz data were obtained from the Sunspot Index and Long-term Solar Observations (SILOS) with website (<https://www.sidc.be/SILSO/datafiles>).

The downloaded and processed h'F2 data are presented depending on the local time (LT) of the observation stations and are calculated in terms of the coordinated universal time (UTC) using the relation in ~~Equations~~ 1a and 1b.

$$LT = UTC + HD \quad (1a)$$

if the station is ahead of UTC.

$$LT = UTC - HD \quad (1b)$$

if UTC is ahead of the station, where HD is hour difference.

For Ilorin station, ~~equation~~ Equation 1a was applied because Ilorin is 1 hour ahead of UTC while for Boa Vista, ~~Equation~~ 1b ~~was~~ applied because Boa Vista is 4 hours behind of UTC.

2.2 Method of analysis

Analysis ~~were~~ ~~was~~ carried out by first finding the hourly monthly mean values of the h'F2 data using the statistical mean relation shown in ~~equation~~ Equation 2. Secondly, the data were grouped into four different seasons comprising ~~of~~ three months each and were averaged to obtain their mean seasonal values using ~~equation~~ Equation 3. The seasons are December solstice (November, December and January), March equinox (February, March and April), June solstice (May, June, and July), and September equinox (August, September and October).

Furthermore, annual mean values of h'F2 for the two years under investigation were evaluated using ~~equation~~ Equation 4

$$\text{Monthly Mean } h'F2 = \frac{1}{n} \sum_i^n h'F2_i \quad (2)$$

where n is the number ~~of~~ ~~of~~ hourly data present in a month.

$$\text{Seasonal Mean } h'F2 = \frac{1}{3} \sum_i^3 h'F2_i \quad (3)$$

$$\text{Annual Mean } h'F2 = \frac{1}{12} \sum_i^{12} h'F2_i \quad (4)$$

Thereafter, the analyzed h'F2 data were plotted against the local time of the stations during minimum and ascending phases ~~of~~ ~~of~~ solar cycle 25 to investigate their variations.

3. RESULTS AND DISCUSSION

3.1 Diurnal and Seasonal Variation of h'F2 at Ilorin during ~~M~~ minimum ~~p~~ phase of ~~solar~~ Solar cycle ~~Cycle~~ 25

Depicted in Figs.1 and 2 below are the plots of the diurnal and seasonal variation of h'F2 at Ilorin and Boa Vista during ~~the~~ minimum phase (year 2020) of solar cycle 25 for the different seasons against ~~local time (LT)~~ LT respectively. From Figs.1 and 2, all the plots followed the same trend and were characterized by similar diurnal features of the h'F2 variation with ~~local time (LT)~~ LT, showing low values at ~~pre-noon~~ pre-noon and ~~post-noon~~ post-noon periods, with ~~the~~ highest peak values observed before or around noon as expected due to the lifting up of the F2-layer height as a result of ~~a~~ high level of ionization during such period. This phenomenon can be attributed to the primary mechanism behind ionosphere formation, which is the photo-ionization of neutral species in the upper atmosphere by solar radiation. While other factors also contribute to ionization modification, photo-ionization predominates

during daytime hours. At nighttime, the ionosphere in this region is predominantly influenced by transport and loss processes. This observation underscores the typical equatorial ionosphere characteristics over Ilorin and Boa Vista. In the F2-layer, particularly in equatorial regions, the vertical drift of ionization due to $E \times B$ force and neutral wind becomes notably influential. Consequently, this leads to deviations in electron density morphology from the expectations of a simple Chapman-type theory [35].

Further observation from the plots revealed two typical night peaks; post-midnight peak (05:00 LT) and ~~pre-midnight~~pre-midnight peak (20:00 LT)

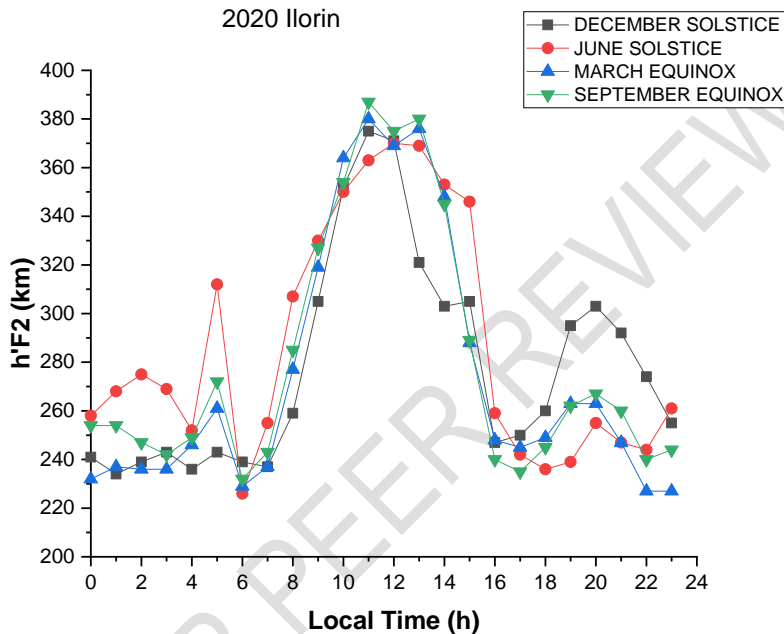


Fig. 1: Diurnal and seasonal variation of h'F2 at Ilorin during minimum phase year 2020 of solar cycle 25

Diurnally, the h'F2 variation appears to be lower at ~~pre-noon~~pre-noon period 0:00 – 06:00 LT except at 05:00 LT where the h'F2 recorded a slight peak value of 312 km (post-midnight peak). At post noon period (18:00 - 23:00 LT) the h'F2 is also low except at 20:00 LT where the virtual height is raised to a peak value of 303 km (pre-midnight peak). The occurrence of two distinct nighttime peaks, observed around 05:00 LT and 20:00 LT respectively, can be attributed to sudden electron density gradients induced by the initiation and cessation of solar ionization, along with the superimposition of spread F on the background electron density [36]. During the noon period, the highest height values of 387 km and 380 km of the h'F2 variations were observed at 11: 00 LT (morning peak or pre-noon peak) and at 14:00 LT (afternoon peak or ~~post-noon~~post-noon peak). This can be attributed to the influence of solar ionization and the effect of $E \times B$ force on F2-layer plasma since a high level of ionization of free electrons can be observed during the day, especially during local noon. During the night, this concentration decreases, but the layer remains due to low recombination of highest concentration ion with neutral wind transport effects. The equatorial

meridional wind also plays an important role in the nighttime F2-layer ion density maintenance [8]; [13]; [15].

Under the seasonal consideration, the variation of h'F2 was observed to be highest (i.e. 312 km) at-duringthe pre-noon period during June solstice at 05:00 LT. At around noon, the highest peak value of 387 km was observed during September equinox. While at post-noon period the highest height value of 303 km was observed during December solstice at 20:00 LT. The lowest peak value of 232 km of h'F2 variation was observed at 06:00 LT during June solstice

3.2 Diurnal and Seasonal Variation of h'F2 at Boa Vista during Minimum Phase Year 2020 of Solar Cycle 25

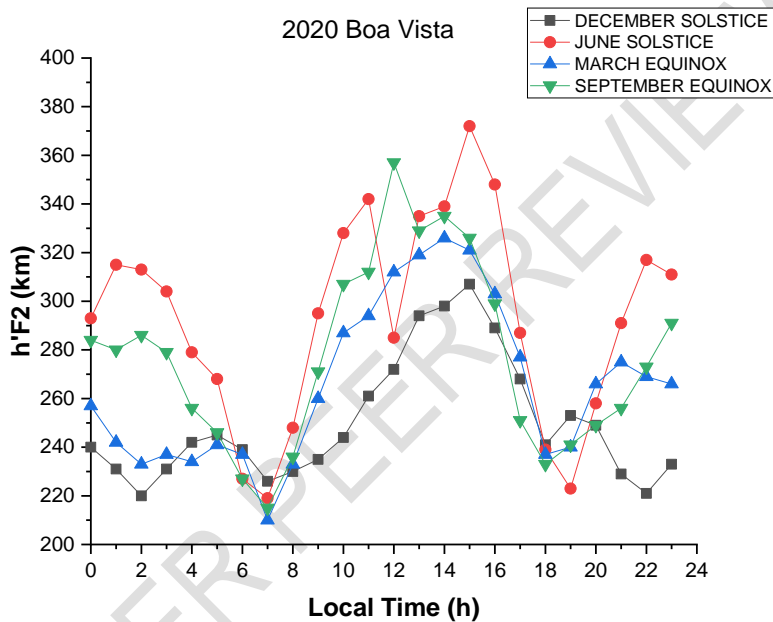


Fig. 2: Same as Fig. 1 but at Boa Vista station

At Boa Vista station, during the minimum phase year 2020 of solar cycle 25, the diurnal variation from Fig. 2 revealed lower values of h'F2 variations at pre-noonpre-noon period 0:00 – 06:00 LT except at 01:00 LT where the h'F2 recorded a high peak value of 315 km (post-midnight peak). At post noon period (18:00 - 23:00 LT) the h'F2 values are also low except at 22:00 LT where the virtual height is raised to a peak value of 317 km (pre-midnight peak). During the noon period, the h'F2 variation had the highest peak values of 357 km at 12:00 LT and 372 km during post noon-post-noon period at 15:00 LT (afternoon peak or post-noonpost-noon peak).

For the seasonal variations of the h'F2 at Boa Vista station, June solstice recorded a peak value of 315 km at 01:00 LT during the post-midnight period, 357 km during September equinox at 12:00 LT (noon period). During post-noonthe post-noon period, h'F2 had two highest peak values of 372 km and 317 km at 15:00 LT and 22: 00 LT respectively, during June solstice. The lowest h'F2 value of 215 km was seen at 07:00 LT during March equinox.

Observations from Figs 1 and 2 showed that the h'F2 variations were higher at Ilorin than at Boa Vista during minimum phase of solar cycle 25.

3.3 Diurnal and Seasonal Variation of h'F2 at Ilorin during Ascending phase Phase year-2021 of Solar Cycle 25

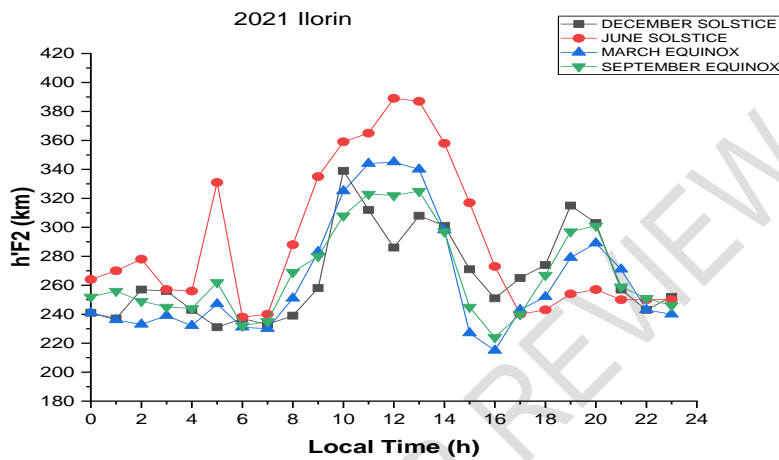


Fig. 3: Diurnal and seasonal variation of h'F2 at Ilorin station during ascending phase year 2021 of solar cycle 25

From Fig. 3 at Ilorin station and during ascending phase (year 2021) of solar cycle 25, the diurnal variations of h'F2 were observed to be lower at pre-pre-noon period (0:00 – 06:00 LT) except during 05:00 LT where a high peak value of 331 km (post mid-night peak) was observed. At the noon period (12:00 – 13:00), the two highest peak values of h'F2 (389 km and 387 km) were observed at 12:00 LT (noon) and 13:00 LT (afternoon or post-noon peak) respectively. During post noon period (18:00 -23:00 LT) the h'F2 values were low except at 19:00 LT where the virtual height recorded a high peak value of 315 km (pre-midnight peak).

Seasonally, the June solstice has the highest virtual height of 389 km during the noon period (12:00 LT) and 331 km during the pre-noon (05:00 LT) respectively. During the post-noon period, the highest h'F2 value of 315 km was recorded during the December solstice at 19:00 LT. While the least h'F2 value of 218 km was observed at 16:00 LT.

3.4 Diurnal and Seasonal Variation of h'F2 at Boa Vista during ascending phase 2021 Ascending Phase of Solar Cycle 25

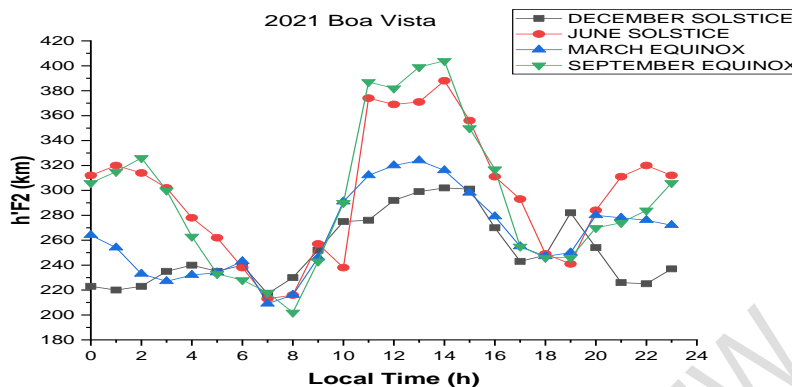


Fig. 4: Same as Fig. 3 but at Boa Vista station

From Fig. 4 above, the diurnal variation of h'F2 during the ascending phase (year 2021) of solar cycle 25, showed high peak values of 326 km during pre-noon at 02:00 LT (post-midnight peak), 387 km at 11:00 LT (morning peak or pre-noon peak). During ~~post-noon~~ post-noon periods, peak values of 404 km and 320 km of h'F2 variations were observed at 14:00 LT (afternoon peak or ~~post-noon~~ post-noon peak) and 22:00 LT (pre-midnight peak) respectively.

On Seasonally view, the variation of h'F2 at Boa Vista station revealed that September equinox had the highest peak values of 326 km at 02:00 LT during the pre-noon period, 387 km at noon and 404 km at 14:00 LT during the post-noon period respectively, and 320 km during June solstice at 22:00 LT. From Figs. 3 and 4, it is clear that h'F2 has ~~high-a~~ higher variation at Boa Vista than at Ilorin during the ascending phase of cycle 25. The lowest h'F2 value of 202 km was observed during September equinox at 08:00 LT.

The diurnal variation profiles of h'F2 at Ilorin and Boa Vista exhibit slight differences across seasons. At both stations, the profile resembles a dome shape, occasionally featuring two distinct peaks: one in the morning between 10:00 – 11:00 LT (pre-noon peak) and another ~~in the afternoon between 13:00 – 14:00~~ between 13:00 – 14:00 LT (post-noon peak), with a midday depression known as noon bite out (NBO) or plateau. These variations stem from diverse dynamics at the equator and the crests of the equatorial ionization anomaly (EIA). The observed plateau and dome shapes are attributed to the relatively weak equatorial electrojet signature induced by the E x B drift [37 - 38]. The combined effect of the Earth's electric and magnetic fields contributes to vertical ionization drift around the equator, resulting in daytime ionization depletion, particularly around noon. Furthermore, the geographical positioning of the stations relative to the magnetic equator plays a role [39]. Boa Vista, situated at latitude 2.80°N, lies on the equatorial anomaly region's border, characterized by highly variable dynamics, while Ilorin, positioned at latitude 14.80°N, resides in the northern hemisphere near the equatorial anomaly crest.

Previous investigations into F2-layer climatology during sunspot cycles 20, 21, and 22 were conducted by [40], at Ibadan, Singapore and Slough, [41] at Phu Thuy, and [42] at Ouagadougou, situated near the magnetic equator. These studies revealed similar variations in ionospheric behaviour observed.

3.5 Annual Variation of h'F2 at Ilorin and Boa Vista during ~~minimum~~ Minimum phase ~~Phase~~ of solar ~~Solar cycle~~ Cycle 25

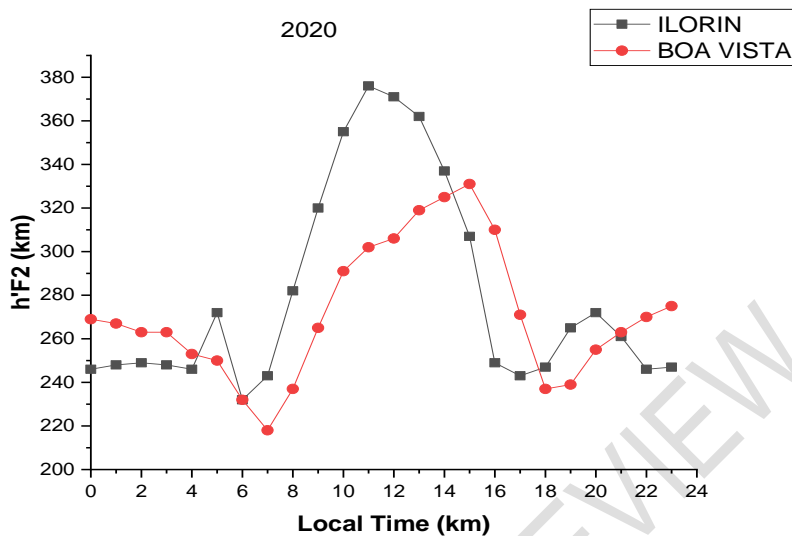


Fig. 5: Annual Variation of h'F2 at Ilorin and Boa Vista during minimum phase year 2020 of solar cycle 25

Depicted in Figs. 5 and 6 are the annual variations of h'F2 at Ilorin and Boa Vista stations during minimum and ascending phase years (2020 and 2021 respectively) of solar cycle 25. From Fig. 5 and during minimum phase year 2020 of solar cycle 25, it was observed that the virtual height h'F2 at Ilorin station is greater than that at Boa Vista station. The peak value of the virtual height at Ilorin was observed to be 376 km at 11:00 LT before noon and the lowest value of 232 km was observed during the pre-noon period at 06:00 LT. The peak value of the virtual height at Boa Vista station (331 km) was recorded during the post-noon period at 16:00 LT and the lowest value of 218 km was observed during pre-noon (07:00 LT). This result revealed that the virtual height of F2-layer (h'F2) is greater at Ilorin than at Boa Vista during minimum phase. This may be due to a higher level of ionization at Ilorin compared to that at Boa Vista.

3.6 Annual Variation of h'F2 at Ilorin and Boa Vista during ascending phase of solar cycle 25

Comment [SK2]: Kindly standardize the formatting of the subchapter.

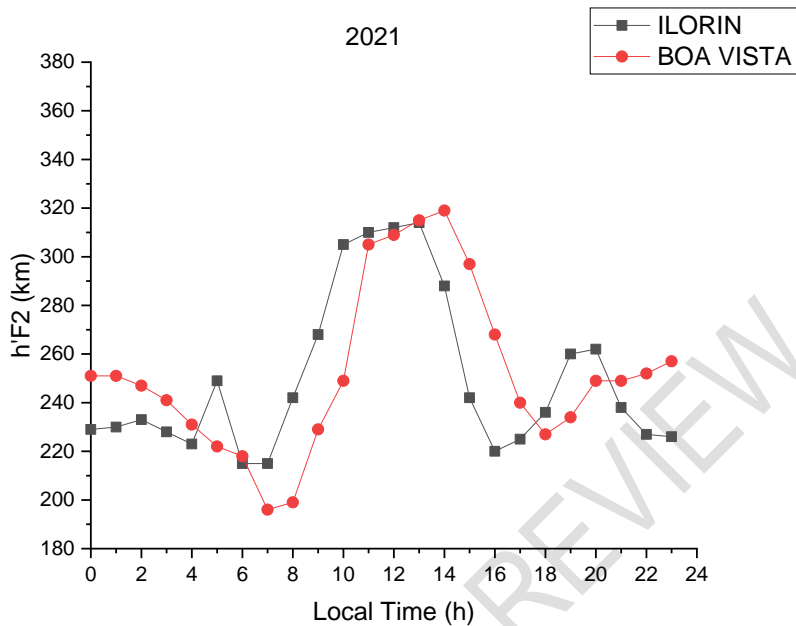


Fig. 6: Annual Variation of h'F2 at Ilorin and Boa Vista during ascending phase year 2021 of solar cycle 25

As seen from Fig. 6 during the ascending phase year 2021 of solar cycle 25, the virtual height at Ilorin and Boa Vista stations are almost the same at around noon period (11:00 – 12:00 LT) and post-noon period (13:00 - 14:00 LT) having a flat ~~plateau-like~~ plateau-like shape. The peak value of the virtual height at Ilorin was observed to be 305 km at 12:00 LT (noon period) and the lowest value of 220 km at 16:00 LT was observed during post noon period. The peak value of the virtual height at Boa Vista station was recorded as 319 km at 15:00 LT during post noon period and the ~~least-lowest~~ least value of 196 km was observed during pre-noon (07:00 LT). Observation from above shows that the variation of the virtual height at Boa Vista is slightly greater than that at Ilorin during the ascending phase. As earlier ~~explain~~ explained this may be ascribed to a higher level of ionization at Boa Vista compared to that at Ilorin.

Comment [SK3]: Kindly check this formatting. Supposed post-noon. Refer to the corrected above.

4.0 Discussion

In the equatorial region, the interaction between the electric field (E) and the Earth's magnetic field (B) generates the $E \times B$ force, which induces vertical ionization drift. During daytime hours (06:00 – 18:00 LT), the $E \times B$ force acts upward, leading to plasma upward drift, whereas during nighttime (18:00 – 05:00 LT), it acts downward, causing plasma to drift downward. Research has demonstrated that the vertical drift velocity varies with season and the phase of the solar cycle [43 – 44]. Especially in the F2-layer heights of the equatorial region, the combined effect of vertical ionization drift by $E \times B$ force and neutral wind significantly shapes electron density morphology, deviating from the expectations of a simple Chapman-type theory. The peculiar variations observed in electron density within the F2-layer, such as pre-noon and post-noon peaks, noon bite out, post-sunset minimum, and nighttime peaks, can be attributed to the influence of neutral winds and the $E \times B$ force on plasma [45 – 48].

Furthermore, higher variability values observed in F2-layer virtual heights during daytime result from the complex nature of F2-layer height variation driven by $E \times B$ force. Nighttime

enhancement of the F2-layer height in this region is primarily influenced by transport and loss processes, as well as gravity waves, which enhance ionospheric electron density gradients. During nighttime, the vertical drift initially exhibits an upward enhancement around 19:00 LT, known as the evening time pre-reversal vertical enhancement (PRE), followed by a downward reversal. The PRE phenomenon, mainly driven by eastward electric fields, significantly alters the F2-layer height and contributes to the evening resurgence of the equatorial ionospheric anomaly (EIA) [35]; [49]. Understanding PRE and pre-noon plasma drift better would offer clearer insights into h'F2 ionospheric variability. The post-noon peak in upward plasma drift signals a rapid depletion of electrons from the equatorial ionosphere F2-layer height, leading to a sharp drop in h'F2 immediately after sunset.

Observation from this research ~~reveal-reveals~~ that Ilorin and Boa Vista data showed unusual features, especially during the nighttime periods that require further investigations. This may be attributed to the volume of data available for analysis in the research and other ~~elertodynamic-electrodynamic~~ factors. Therefore, the analysis of a larger volume of data from these two stations, will be necessary to establish a stronger characterization of its ionospheric h'F2 variation.

5.0 CONCLUSION

This study investigates the diurnal, seasonal, and annual variations in the virtual height of the ionospheric F2-layer over two equatorial stations situated in the African and American longitudinal sectors during the minimum (year 2020) and ascending (year 2021) phases of solar cycle 25. Utilizing data from ionosonde stations located in Ilorin (14.80°N, 17.40°W) and Boa Vista (2.80°N, 299.30°E), the research reveals that ionospheric h'F2 exhibits greater responsiveness to daytime variability (06:00 – 18:00 LT) compared to nighttime (18:00 – 05:00 LT). Seasonally, the highest peak values were observed before noon and ~~post-noon~~ ~~post-noon~~ periods during both minimum and ascending phases of solar activity. For instance, during the minimum phase (year 2020), peak values of 387 Km at 11:00 LT during September equinox (Ilorin) and 372 Km at 15:00 LT during June solstice (Boa Vista) were recorded. Conversely, during the ascending phase (year 2021), peak values were observed at noon and ~~post-noon~~ ~~post-noon~~ periods, with values of 389 Km at 12:00 LT during June solstice (Ilorin) and 404 Km at 14:00 LT during September equinox (Boa Vista). Annually, the highest h'F2 peak values during the minimum phase of solar activity (2020) were recorded at noon, with 376 Km and 302 Km at Ilorin and Boa Vista respectively, while during the ascending phase, both stations recorded almost equal values of 305 km at noon. Overall, h'F2 variation exhibited a higher magnitude at Ilorin in the African longitudinal sector than at Boa Vista in the American longitudinal sector during the minimum phase of solar cycle 25, with the reverse observed during the ascending phase.

REFERENCES

1. Bora, S. Ionosphere and radio communication. Resonance. 2017; 22(2): 123-133.
2. Atiq M. Historical review of ionosphere in perspective of sources of ionization and radio waves propagation. Research & Reviews: Journal of Space Science & Technology. 2018; 7(2): 28.
3. Shiokawa K. Introduction of Space Weather Research on Magnetosphere and Ionosphere of the Earth. In Solar-terrestrial environmental prediction Singapore: Springer Nature Singapore. 2023; 95-113.
4. Yusuf Olanrewaju Kayode, Eugene Onori, Oluwafunmilayo Ometan, Sakiru Abiodun Okedeyi, Anthony Segara Ajose, Rafiu Bolaji Adegbola, Rasaq Adewemimo Adeniji-Adele. Total Electron Content Variations at a LowLatitude East African Station and Its Comparison with IRI-2016, IRI-Plas2017 and NeQuick-2 Models during Solar

Cycle 24. International Journal of Recent Research in Physics and Chemical Sciences. .2023a; 10(2): 13-40.

DOI: <https://doi.org/10.5281/zenodo.10254820>

5. Yusuf Kayode, Eugene Onori, Emmanuel Somoye, Aghogho Ogwala, Razaq Adeniji-Adele. The Assessments of the Performances of IRI-2016, IRI-Plas2017 and NeQuick-2 models Using GPS-TEC at an Australian Global Positioning Systems (GPS) Station during Solar Cycle 24. Journals of Research and Review in Sci. (2023b); 10: 75-93. DOI:10.36108/jrrslasu/3202.01.0111
6. Amaechi PO, Oyeyemi EO, Akala AO, Kaab M, Younas W, Benkhaldoun Z, et al. Comparison of ionospheric anomalies over African equatorial/low-latitude region with IRI-2016 model predictions during the maximum phase of solar cycle 24. Advances in Space Research. 2021; 68(3): 1473-1484.
7. Ribeiro BAG, Fagundes PR, Venkatesh K, Tardelli A, Pillat VG, & Seemala GK. Equatorial and low-latitude positive ionospheric phases due to moderate geomagnetic storm during high solar activity in January 2013. Advances in Space Research. 2019; 64(4): 995-1010.
8. Somoye EO, Akala AO, Adeniji-Adele RA, Iheonu EE, Onori EO, Ogwala A. Equatorial F2 characteristic variability: A review of recent observations. Advances in Space Research. 2013; 52: 1261–1266
9. Bakr EF, Zaki WH, & Mohammed JH. The effect of sunspots number on critical frequencies fof2 for the ionospheric layer-f2 over kirkuk city during the ascending phase of solar cycle 24. Kirkuk University Journal-Scientific Studies. 2021; 16(3): 19-27.
10. Onori Eugene O, Ometan Oluwafunmilayo O, Adeniji-Adele Razaq A, Ogungbe Abiola S, Ogabi Cornelius O, Ogwala Aghogho, et al. Seasonal Response of Peak Electron Density of F2-Layer in the African and American Sectors during Low Solar Activity Period of Cycle 24. Applied Physics Journal. 2021; 4(1): 1 -10. DOI: <https://doi.org/10.31058/j.ap.2021.41001>
11. Sasmal S, Chowdhury S, Kundu S, Politis DZ, Potirakis SM, Balasis G, et al. Pre-seismic irregularities during the 2020 Samos (Greece) earthquake (M= 6.9) as investigated from multi-parameter approach by ground and space-based techniques. Atmosphere. 2021; 12(8): 1059.
12. Hunsucker RD, & Hargreaves JK. The high-latitude ionosphere and its effects on radio propagation. Cambridge University Press. 2007.
13. Adebesein BO, Adekoya BJ, Ikubanni SO, Adebisi SJ, Adebesein OA, Joshua BW, et al. Ionospheric foF2 morphology and response of F2-layer height over Jicamarca during different solar epochs and comparison with IRI-2012 model; J. Earth Syst. Sci. 2014; 123(4): 751–765.
14. Gurevich AV. Nonlinear effects in the ionosphere. Physics-Usppekhi. 2007; 50(11): 1091.
15. Onori EO; Somoye EO, Ogungbe AS, Ogabi CO, Ogwala A. Longitudinal Influence of NmF2 Variability on the Equatorial Ionosphere during High Solar Activity. Physics Journal. 2015; 3(2): 388-392.
16. Anduaga A. The realist interpretation of the atmosphere. Studies in History and Philosophy of Science Part B: Studies in History and Philosophy of Modern Physics. 2008; 39(3): 465-510.
17. Koucká Knížová P, Laštovička J, Kouba D, Mošna Z, Podolská K, Potužníková K, et al. Ionosphere influenced from lower-lying atmospheric regions. Frontiers in Astronomy and Space Sciences. 2021; 8: 651445.
18. Borchevskina O, Karpov I, & Karpov M. Meteorological storm influence on the ionosphere parameters. Atmosphere. 2020; 11(9): 1017.
19. Elmunim NA, Abdullah M, Elmunim NA, & Abdullah M. Ionosphere. Ionospheric Delay Investigation and Forecasting. 2021; 19-29.

20. Wang B, & Ding Q. Global monsoon: Dominant mode of annual variation in the tropics. *Dynamics of Atmospheres and Oceans*. 2008; 44(3-4): 165-183.
21. Batista MC, Santos ORD, Matins VC, Vieira TF. Teaching Seasons with a Hands-on Activity. *International Astronomy and Astrophysics Research Journal*. 2022; 4(3): 19-35.
22. Stephens GL, & L'Ecuyer T. The Earth's energy balance. *Atmospheric Research*. 2015; 166: 195-203.
23. Louffi A, Pitout F, Bounhir A, Benkhaldoun Z, Makela JJ, Abamni S, et al. Interhemispheric asymmetry of the equatorial ionization anomaly (EIA) on the African sector over 3 years (2014–2016): Effects of thermospheric meridional winds. *Journal of Geophysical Research: Space Physics*. 2022; 127(9): e2021JA029902.
24. Balan N, Liu L, Le H. A brief review of equatorial ionization anomaly and ionospheric irregularities. *Earth and Planetary Physics*. 2018; 2(4): 257-275.
25. Oluwadare TS, Thai CN, Akala AO, Heise S, Alizadeh M, Schuh M. Characterization of GPS-TEC over African equatorial ionization anomaly (EIA) region during 2009–2016. *Advances in Space Research*. 2019; 63(1): 282-301.
26. Abdu MA. Equatorial ionosphere–thermosphere system: Electrodynamics and irregularities. *Advances in Space Research*. 2005; 35(5): 771-787.
27. Essien P, Figueiredo CA, Takahashi H, Wrasse CM, Barros D, Klutse NAB et al. Long-term study on medium-scale traveling ionospheric disturbances observed over the South American Equatorial Region. *Atmosphere*. 2021; 12(11): 1409.
28. Hathaway DH. The solar cycle. *Living reviews in solar physics*. 2015; 12(1): 4.
29. Moussas X, Polygiannakis JM, Preka-Papadema P, Exarhos G. Solar cycles: A tutorial. *Advances in Space Research*. 2005; 35(5): 725-738.
30. Lockwood M, Owens M, Barnard L, Davis C, Thomas S. Solar cycle 24: what is the Sun up to?. *Astronomy & Geophysics*. 2012; 53(3): 3-9.
31. Broomhall AM, Chatterjee P, Howe R, Norton AA, Thompson MJ. The Sun's interior structure and dynamics, and the solar cycle. *Space Science Reviews*. 2014; 186: 191-225.
32. Charbonneau P. Solar dynamo theory. *Annual Review of Astronomy and Astrophysics*. 2014; 52: 251-290.
33. Maddanu F & Proietti T. Modelling persistent cycles in solar activity. *Solar Physics*. 2022; 297(1): 13.
34. Bocchialini K, Grison B, Menvielle M, Chambodut A, Cornilleau-Wehrlin N, Fontaine D, et al. Statistical analysis of solar events associated with storm sudden commencements over one year of solar maximum during cycle 23: Propagation from the Sun to the Earth and effects. *Solar Physics*. 2018; 293(5): 75.
35. Oladipo AO, Adeniyi JO, Radicella SM, Adimula I A. Variability of the ionospheric electron density at fixed heights and Validation of IRI- 2007 profiles prediction at Ilorin. *Adv. Space Res*. 2011; 47: 496 – 505.
36. Chou YT and Lee CC. Ionospheric variability at Taiwan low latitude station: Comparison between observations and IRI 2001 model. *Adv. Space Res*. 2008;. 42: 673 – 681.
37. Faynot JM. and villa P. F-Region at the Magnetic Equator. *Annals of Geophysics*. 1979; 35: 1- 9.
38. Gnabahou D A, Ouattara F, Nanéma E, Zougmoré F. foF2 Diurnal Variability at African Equatorial Stations: Dip Equator Secular Displacement Effect. *International Journal of Geosciences*. 2013; 4: 1145 – 1150.
39. Forbes JM, Palo SE, Zhang X. Variability of the ionosphere. *Journal of Atmospheric and Solar-Terrestrial Physics*. 2000; 62: 685 – 693.

40. Somoye EO, Akala AO, Ogwala A. Day to day variability of h'F and foF2 during some solar cycle epochs. *Journal of Atmospheric and Solar-Terrestrial Physics*. 2011; 73: 1915–1922.
41. Pham Thi Thu H, Amory-Mazaudier C and Le Huy M. Time variations of the ionosphere at the northern tropical crest of ionization at Phu Thuy, Vietnam. *Ann. Geophys.* 2011; 29: 197–207. doi:10.5194/angeo-29-197-2011
42. Quattara F and Amory-Mazaudier C. Statistical study of the equatorial F2-layer critical frequency at Ouagadougou during solar cycles 20, 21, and 22 using Legrand and Simon's classification of geomagnetic activity. *J. Space Weather Space Clim.* 2012; 2(A19): 1- 9. DOI: 10.1051/swsc/2012019.
43. Fejer BG, Farley DT, Woodman RF, Calderon C. Dependence of Equatorial F-Region Vertical Drifts on Season and Solar Cycle. *Journal of Geophysical Research*. 1979; 84(A10): 5792.
44. Fejer BG. Low latitude ionospheric electrodynamics. *Space Sci. Rev.* 2011; 158 (1): 145 – 166.
45. Rajaram G and Rastogi R.G. Equatorial electron densities – Seasonal and solar cycle changes. *J. Atmos. Terr. Phys.* 1977; 39: 1175–1182.
46. Radicella SM and Adeniyi JO. Equatorial ionospheric electron density below the F2 peak. *Radio Sci.* 1991; 34(5): 1153 – 1163.
47. Lee CC, Reinisch, BW. Quiet-condition hmF2, NmF2, and B0 variations at Jicamarca and comparison with IRI-2001 during solar maximum. *J. Atmos. Sol. Terr. Phys.* 2006; 68: 2138–2146.
48. Lee CC, Reinisch BW, Su SY, Chen WS. Quiet-time variations of F2-layer parameters at Jicamarca and comparison with IRI-2001 during solar minimum. *J. Atmos. Sol. Terr. Phys.* 2008; 70: 184–192.
49. Sumod SG, Pant TK, Lijo Jose, Hossain MM, Kumar KK. Signatures of Sudden Stratospheric Warming on the Equatorial Ionosphere-Thermosphere System. *Planetary and Space Science*. 2012; 63(64): 49–55.